ISSN 1070-3284, Russian Journal of Coordination Chemistry, 2017, Vol. 43, No. 4, pp. 252–259. © Pleiades Publishing, Ltd., 2017.

Crystal Structures and Enhanced Luminescence of Zn(II) and Cd(II) Complexes Containing Conjugated Organic Ligands[1]

L. Sun, W. X. Zhang, J. Ma, Y. L. Gao, N. Xu, C. Y. Pan, T. Q. Lu, X. Y. Hu, and F. Jin*

Department of Chemistry and Chemical Engineering, Fuyang Normal College, Fuyang, 236037 P.R. China

**e-mail: jflyw@163.com*

Received March 25, 2016

Abstract– By self-assembly of delocalized organic ligands (L^1 and L^2) with $Cd(SCN)_2$, ZnI_2 and $Zn(NCS)_2$, three luminescent complexes $ZnI_2(L^1)_2$ (**I**), $[Cd(L^1)_2(\mu_{1,3}\text{-}SCN)_2]_n$ (**II**) and $Zn(NCS)_2(L^2)_2$ (**III**) were obtained (L^1 = 2-{5,5-dimethyl-3-[2-(pyridine-4-yl)ethenyl]cyclohex-2-enylidene}propanedinitrile and L^2 = 2-{5,5-dimethyl-3-[2-(pyridine-3-yl)ethenyl]cyclohex-2-enylidene}propanedinitrile). The structures of the complexes were determined by single crystal X-ray diffraction analysis (CIF files CCDC nos. 1406116 (**I**), 1406115 (**II**), and 1400360 (**III**)). In complex **I**, Zn(II) is coordinated by two functional organic ligands and two I^- ions, to form a I_2N_2 distorted tetrahedral geometry. In 1D coordination polymer **II**, the Cd(II) centers show six-coordinated geometries, two organic ligands and four SCN^- ions involve in coordination with each Cd(II) center. The thiocyanate groups show $\mu_{1,3}$-SCN bridging coordination modes and the adjacent Cd(II) ions are bridged by double $\mu_{1,3}$-SCN ions to form an infinite chain. In complex **III**, Zn(II) is coordinated by two functional organic ligands and two NCS^- groups, to form a N_4 distorted tetrahedral geometry. Compared with the free ligands, the complexes show superior luminescent property with red-shift and enhancement of fluorescence intensity.

Keywords: self-assembly, Zn(II) complex, Cd(II) complex, crystal structure, luminescent property

DOI: 10.1134/S1070328417040078

INTRODUCTION

In recent years, design and synthesis of inorganic-organic hybrid complexes have become one of the most active fields due to their fascinating structural diversities, special properties, and potential applications as functional materials [1–9]. In coordination compounds, the metal ions can act either as a multidimensional template for increasing the molecular number density of functional organic ligand, or as an important structural control on the intramolecular charge transfer process, leading to more excellent fluorescent properties [10–12]. Zn(II) and Cd(II) have closed-shell electronic configuration. Complexes based on zinc(II) and cadmium(II) ions can be anticipated to produce excellent fluorescence characteristics dependent on the ligands. Therefore, luminescent Zn(II) and Cd(II) complexes are of increasing interest in photochemistry, luminescence sensors, optical probes, and so on [12–16].

In our previous work, two isophorone-based ligands, namely, 2-{5,5-dimethyl-3-[2-(pyridine-4-yl)ethenyl]cyclohex-2-enylidene}propanedinitrile (L^1) and 2-{5,5-dimethyl-3-[2-(pyridine-3-yl)ethenyl]cyclohex-2-enylidene}propanedinitrile (L^2) have been synthesized and successfully used to construct a series of diverse structural Ag(I) complexes. Compared with the ligands, the Ag(I) complexes show superior luminescent properties [6, 8]. In order to obtain new fluorescent materiales and further study the influence of different metal ions on the optical properties of the complexes, self-assembly of L^1 and L^2 with Zn(II) and Cd(II) salts was presented.

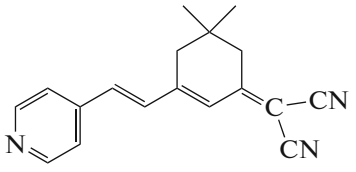

(L1)

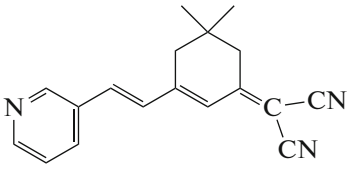

(L2)

[1] The article is published in the original.

Herein, we report the syntheses, crystal structures and luminescent property of three complexes $ZnI_2(L^1)_2$ (**I**), $[Cd(L^1)_2(\mu_{1,3}\text{-}SCN)_2]_n$ (**II**) and $Zn(NCS)_2(L^2)_2$ (**III**).

EXPERIMENTAL

Materials and physical measurements. All commercially available chemicals are of analytical grade and were used without further purification. The ligands were synthesized using our strategy reported earlier [6, 8]. Elemental analyses were carried out on a Perkin-Elmer 240 analyzer. The IR spectra were recorded from KBr discs in the 4000–40 cm^{-1} range on a nicolet Nexus 870 spectrophotometer. The solid state luminescence spectra were measured on a Hitachi F-7000 fluorescence spectrophotometer. In the measurements of emission and excitation spectra, the pass width is 5 nm for the compounds.

Synthesis of complex I. A clear methanol solution (20 mL) of ZnI_2 (0.32 g, 1 mmol) was carefully layered onto a solution of L^1 (0.55 g, 2 mmol) in dichloromethane (15 mL). The yellow flake crystals of complex I suitable for single crystal X-ray diffraction were obtained by slow interlayer diffusion. The yield was 0.69 g (79%).

For $C_{36}H_{34}N_6I_2Zn$			
anal. calcd., %:	C, 49.71;	H, 3.94;	N, 9.66.
Found, %:	C, 49.30;	H, 3.36;	N, 9.98.

IR bands (ν, cm^{-1}): 2968 m, 2220 s (−C≡N), 1570 s, 1539 s, 1385 s, 1332 s, 971 s, 695 s.

Synthesis of complex II. The reaction procedure was carried out in the similar manner above, except that $Cd(SCN)_2$ (0.23 g, 1 mmol) was used instead of ZnI_2. The yellow needle crystals of complex **II** suitable for single crystal X-ray diffraction were obtained. The yield was 0.51 g (72%).

For $C_{38}H_{34}N_8S_2Cd$			
anal. calcd., %:	C, 58.57;	H, 4.40;	N, 14.38.
Found, %:	C, 58.92;	H, 4.01;	N, 14.89.

IR bands (ν, cm^{-1}): 2964 m, 2225 s (−C≡N), 2126 s (NCS), 1568 s, 1541 s, 1386 s, 1329 s, 976 s, 692 s.

Synthesis of complex III. The reaction procedure was carried out in the similar manner above, except that $Zn(SCN)_2$ (0.18 g, 1 mmol) was used instead of ZnI_2, and L^2 (0.36 g, 2 mmol) was used instead of L^1. The yellow rod-like crystals of the complex suitable for single crystal X-ray diffraction were obtained. The yield was 0.51 g (69%).

For $C_{38}H_{34}N_8S_2Zn$			
anal. calcd, %:	C, 62.33;	H, 4.68;	N, 15.30.
Found, %:	C, 62.01;	H, 4.26;	N, 15.79.

IR bands (ν, cm^{-1}): 2964 m, 2227 s (−C≡N), 2081 s (NCS), 1574 s, 1539 s, 1387 s, 1334 s, 972 s, 694 s.

X-ray crystallography. Diffraction intensities were collected on a Bruker SMART CCD area detector using graphite monochromated MoK_α radiation (λ = 0.71069 Å) at 298(2) K. Intensity data were collected in the variable ω-scan mode. The structure was solved by direct methods and difference Fourier syntheses. The non-hydrogen atoms were refined anisotropically and hydrogen atoms were introduced geometrically. Calculation was performed with SHELXTL-97 program package [17]. Details of the crystal parameters, data collections and refinements are listed in Table 1, and selected bond distances and angles are given in Table 2.

Supplementary material for structures I–**III** has been deposited with the Cambridge Crystallographic Data Centre (CCDC nos. 1406116 (I), 1406115 (**II**), and 1400360 (**III**); www.ccdc.cam.ac.uk/data_request/cif).

RESULTS AND DISCUSSION

In the conjugated backbone of the organic ligands, the bond distances of C−C and C−N are all shorter than the normal single bond and longer than the normal double bond (Table 2). The normal C−N single bond (1.47 Å), C=N double bond (1.33 Å), C=C double bond (1.34 Å), C−C single bond (1.54 Å) [18]. The facts indicate that there exit extensive electron delocalization in the organic molecules.

The single-crystal X-ray diffraction analysis revealed that complex **I** crystallizes in the orthorhombic system, space group *Aba*2. As depicted in Fig. 1a, the Zn^{2+} ion is located in a distorted tetrahedral geometry and coordinated by two iodine ions and two pyridyl nitrogen atoms from the ligands (Zn−N(1) 2.065(4), Zn−I(1) 2.5351(9) Å). The bond angles for Zn(II) are in the range of 96.0(2)°–122.64(5)°.

As shown in Fig. 1b, the neighboring molecules are linked each other through C(1)−H(1)···I hydrogen bonding interactions to form the 2D structure with H(1)···I distance of 3.12 Å. The 2D supramolecular structures are connected each other through weak C(14)−H(14*A*)···N(3) interactions with H(14*A*)···N(3) distance of 2.67 Å to generate a 3D structure as displayed in Fig. 1c.

Polymer **II** features a 1D polymeric arrangement of formula $[Cd(L^1)_2(\mu_{1,3}\text{-}SCN)_2]_n$ (Fig. 2a). In the chain,

Table 1. Crystallographic data and refinements of complexes **I**–**III**

Parameter	Value		
	I	**II**	**III**
Formula weight	869.86	779.25	732.22
Crystal system	Orthorhombic	Triclinic	Triclinic
Space group	*Aba*2	$P\bar{1}$	$P\bar{1}$
a, Å	9.447(5)	5.845(5)	5.736(5)
b, Å	36.091(5)	8.341(5)	15.244(5)
c, Å	11.234(5)	20.490(5)	22.875(5)
α, deg	90.000(5)	93.742(5)	75.040(5)
β, deg	90	97.988(5)	86.458(5)
γ, deg	90	105.856(5)	85.873(5)
V, Å^3	3830(3)	946(1)	1925(2)
Z	4	1	2
ρ_{calcd}, g cm^{-3}	1.508	1.368	1.263
μ, mm^{-1}	2.284	0.725	0.783
θ Range, deg	1.13–24.99	1.01–27.33	0.92–27.28
Collected reflections	13030	7390	14935
Independent reflections	3266	3765	7614
Refined parameters	206	225	456
R_1, wR_2 ($I > 2\sigma(I)$)	0.0278, 0.0679	0.0217, 0.0647	0.0616, 0.1505
R_1, wR_2 (all data)	0.0361, 0.0849	0.0233, 0.0757	0.1320, 0.1857
GOOF on F^2	1.077	1.003	1.039

the thiocyanate groups show $\mu_{1,3}$-SCN bridging coordination mode through N and S atoms and link two neighboring Cd(II) centers. Each Cd^{2+} ion lies at a center of symmetry surrounded by six related atoms. The equatorial positions are occupied by two nitrogen atoms and two sulfur atoms from four thiocyanate anions and two nitrogen atoms of pyridine groups from two organic ligands occupy the axial positions. Therefore, the polyhedron can be described as a distorted octahedron.

In the crystal structure of polymer **II**, the uncoordinated −C≡N nitrogen atoms play essential roles in generating the 2D supramolecular structure through C−H···N hydrogen bonding interactions. As shown in Fig. 2b, the neighboring chains are connected by C(2)−H(2)···N(2) hydrogen bonding interaction with the H(2)···N(2) distance of 2.60 Å to form 2D sheets.

Single-crystal X-ray diffraction analysis reveals that complex **III** crystallizes in the triclinic space group $P\bar{1}$. As shown in Fig. 3a, in the molecular structure, Zn^{2+} ion is four coordinated by two nitrogen atoms of the pyridyl groups (L) and two nitrogen atoms of thiocyanate anions to form a distorted tetrahedral geometry. The thiocyanate group is coordinated in a linear fashion through the nitrogen atom. The Zn−N bond lengths are in the range of 1.917(4)–2.023(4) Å, which are within the normal range [19,

Table 2. Selected bond lengths (Å) and bond angle (deg) of complexes **I**–**III***

Bond	*d*, Å	Bond	*d*, Å
		I	
Zn(1)–N(1)	2.065(4)	Zn(1)–I(1)	2.5351(9)
C(3)–C(6)	1.462(7)	C(6)–C(7)	1.340(7)
C(8)–C(7)	1.454(6)	C(9)–C(8)	1.345(6)
C(9)–C(10)	1.424(7)	C(16)–C(10)	1.363(8)
		II	
Cd(1)–N(1)	2.364(2)	Cd(1)–S(1)	2.724(1)
Cd(1)–N(4)	2.322(2)	C(4)–C(6)	1.460(3)
C(6)–C(7)	1.331(3)	C(7)–C(8)	1.446(3)
C(8)–C(10)	1.361(3)	C(10)–C(11)	1.432(3)
C(11)–C(16)	1.369(3)		
		III	
Zn(1)–N(1)	1.950(5)	Zn(1)–N(2)	1.916(5)
Zn(1)–N(3)	2.008(4)	Zn(1)–N(4)	2.023(4)
C(5)–C(6)	1.449(6)	C(6)–C(7)	1.321(6)
C(7)–C(8)	1.443(7)	C(10)–C(11)	1.429(7)
C(8)–C(10)	1.333(7)	C(11)–C(16)	1.345(8)
C(20)–C(24)	1.482(6)	C(24)–C(25)	1.290(6)
C(25)–C(26)	1.458(6)	C(26)–C(27)	1.327(7)
C(27)–C(29)	1.419(6)	C(29)–C(34)	1.351(7)
Angle	ω, deg	Angle	ω, deg
		I	
N(1)Zn(1)N(1)$^{\#1}$	96.0(2)	N(1) Zn(1)I(1)	107.73(10)
N(1)$^{\#1}$Zn(1) I(1)	109.72(11)	I(1) Zn(1)I(1)$^{\#1}$	122.64(5)
		II	
N(4)$^{\#1}$Cd(1)N(1)	89.05(7)	N(1) Cd(1)S(1)	91.95(6)
N(4)$^{\#1}$Cd(1)S(1)	85.76(6)		
		III	
N(2) Zn(1)N(1)	115.9(2)	N(7) Zn(1)N(3)	109.6(2)
N(1) Zn(1)N(3)	104.1(2)	N(7) Zn(1)N(4)	110.3(2)
N(1) Zn(1)N(4)	103.1(2)	N(3) Zn(1)N(4)	113.7(2)

* Symmetry transformations used to generate equivalent atoms: $^{\#1}$ $-x + 1, -y + 2, z$ (**I**); $^{\#1}$ $x + 1, y, z$ (**II**).

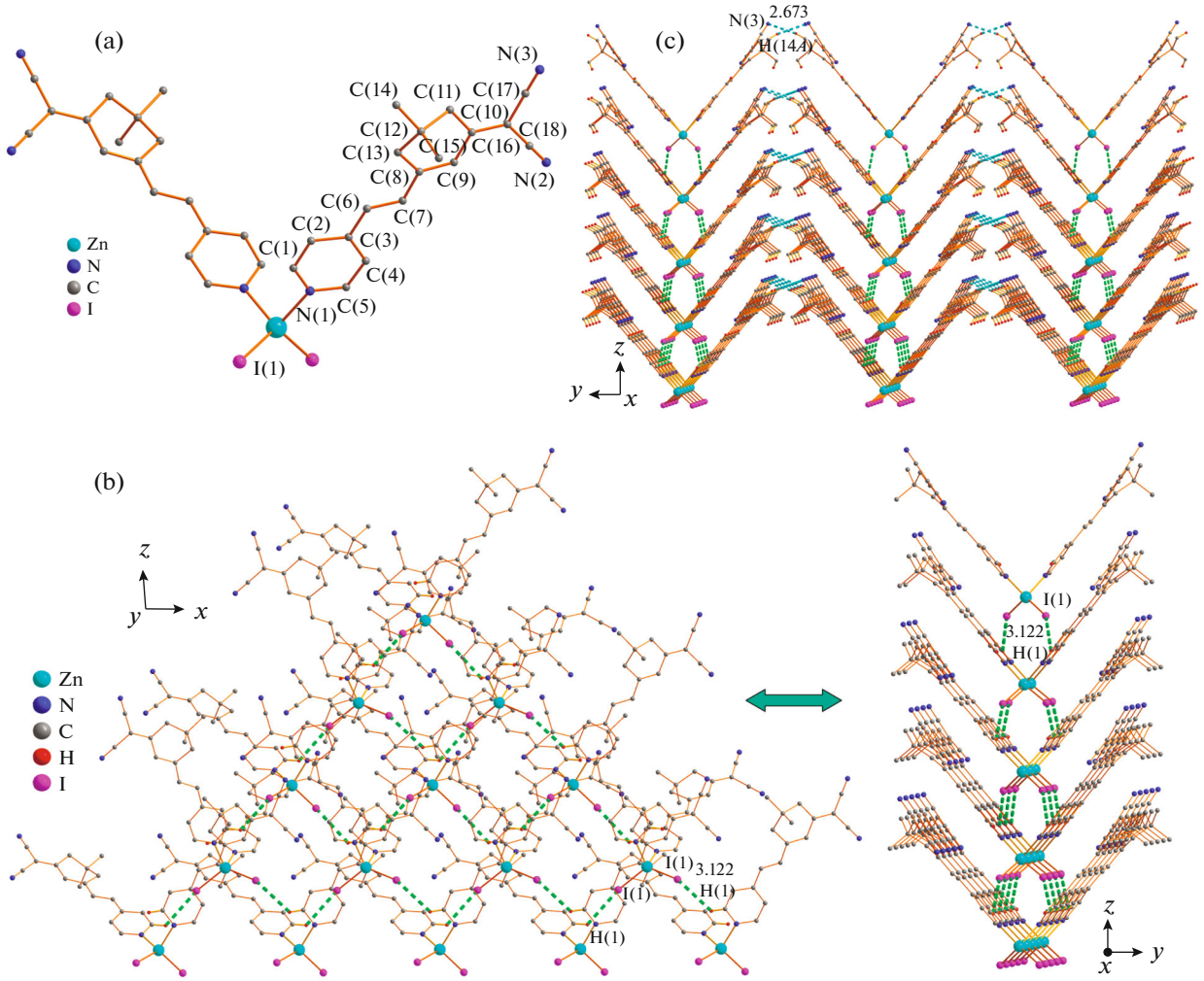

Fig. 1. Molecular structure (a), the 2D structure (b), and the 3D structure of complex **I** (c). The dotted lines represent the weak interactions. Hydrogen atoms not participating in hydrogen bonding are omitted for clarity.

20]. The bond angles around the zinc atom are in the range of 103.1(2)°–115.8(2)°.

As shown in Fig. 3b, the adjacent molecules are linked together by the C(6)–H(6)···π and C(24)–H(24)···π interactions to form a chain with H(6)···C(38) and H(24)···C(38) distances of 2.78(4) and 2.74(4) Å, respectively. The chains are connected each other through C(3)–H(3)···S(2), C(22)–H(22)···N(8) and C(23)–H(23)···N(8) hydrogen bonding interactions to generate the 2D double layer structure (Fig. 3c). As shown in Fig. 3d, the neighboring planes are linked each other through C(14*A*)–H(14*A*)···N(5) hydrogen bonding interactions to form the 3D structure with H(14*A*)···N(5) distance of 2.71(6) Å.

For all complexes, the uncoordinated –C≡N nitrogen atoms play essential roles in generating the high dimensional supramolecular structures through C–H···N hydrogen bonding interactions. In addition, due to the steric hindrance effect of the ring structure and the dimethyl substituents of the organic ligands, no π···π interactions based on organic ligands were observed in the complexes, which would have significant influences on the solid state emission property of the crystals [6, 21–26].

Metal-organic complexes have been reported to have abilities to affect the emission wavelength and intensity of the organic material through metal coordination. Therefore, for potential applications as luminescent materials, the luminescent properties of L^1, L^2 and the complexes have been investigated in the solid state at room temperature upon the optimum excitation wavelength. Figure 4 presents the comparison of the emissiom spectra. Ligands L^1 and L^2 exhibit emission maximum at 517 and 514 nm, respectively, which are assigned to the π-π* transition of the back-

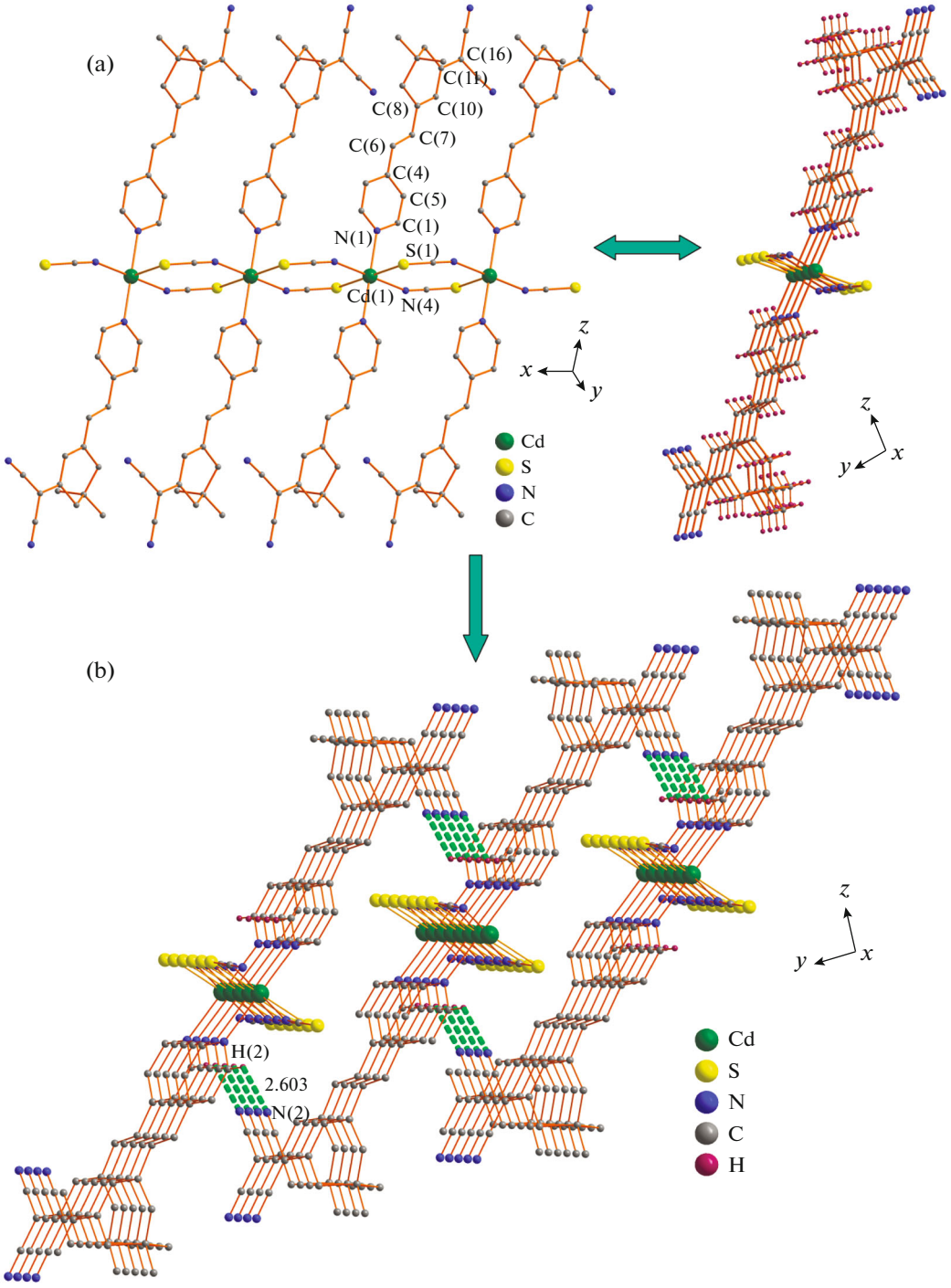

Fig. 2. The 1D (a) and 2D (b) structures of polymer **II**. The dotted lines represent the weak interactions. Hydrogen atoms are omitted for clarity.

bone of the ligands. Compared to those of the ligands, the emission spectra of the complexes **I**–**III** are red-shifted to 547, 548 and 520 nm, respectively, which also derive from the π–π* transition of the coordinated organic ligands [27]. In additional, enhancement of the fluorescence intensity is realized in the complexes. The red shift of the emission band and enhancement of the fluorescence intensity are considered to mainly originate from the coordination of the organic ligands to metal ions. The incorpora-

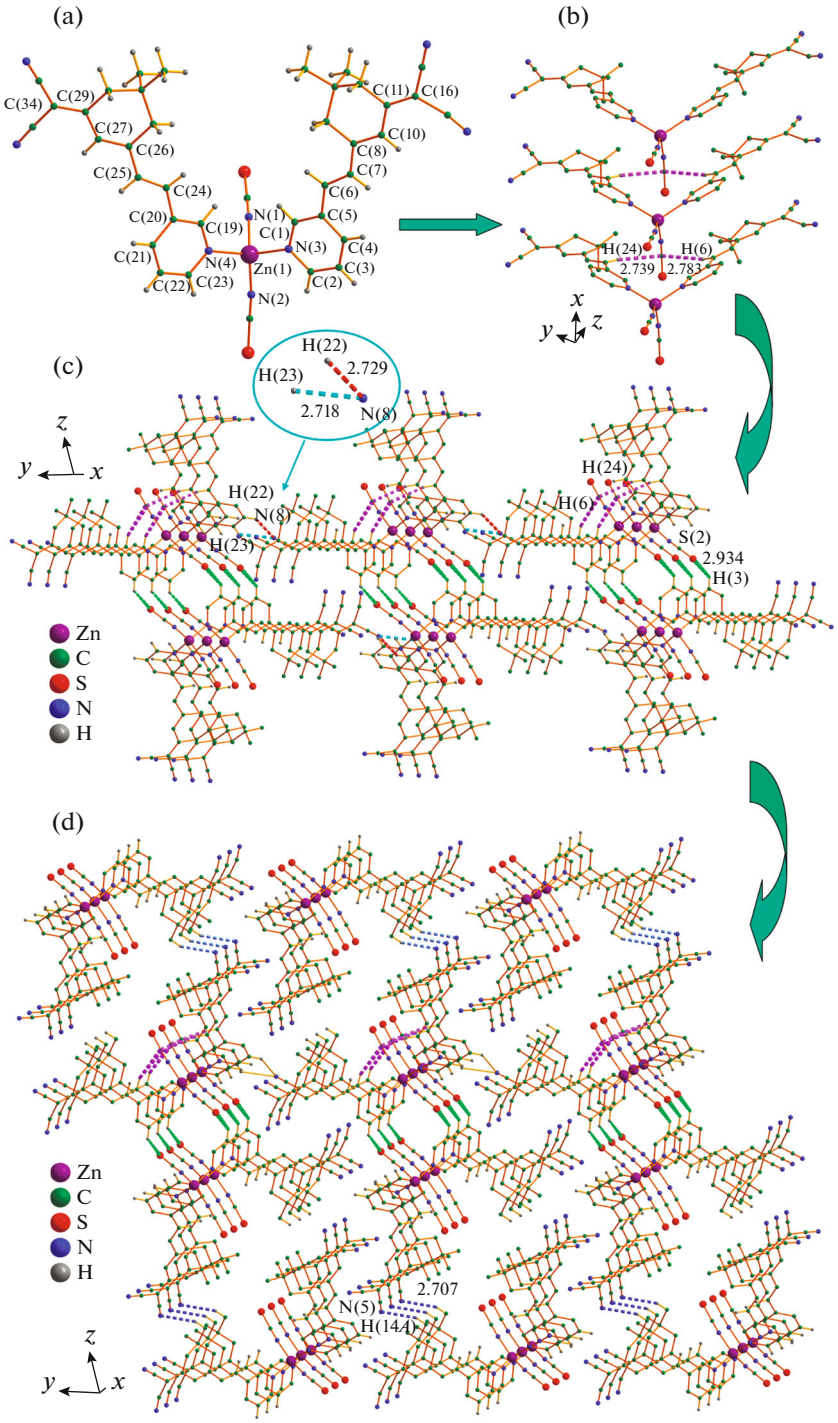

Fig. 3. Molecular structure (a), the 1D structure formed through the C–H···π interaction (b), the 2D double layer structure (c), and the 3D structure of complex **III** (d). The dotted lines represent the weak interactions. Hydrogen atoms not participating in weak interaction are omitted for clarity.

tion of metal ion may increase the conformational rigidity of the organic ligands and reduce the loss of energy via intramolecular vibrational and rotational motions [28].

ACKNOWLEDGMENTS

This work was supported by the National Natural Science Foundation of China (21401024), Natural Science Foundation of Anhui Province

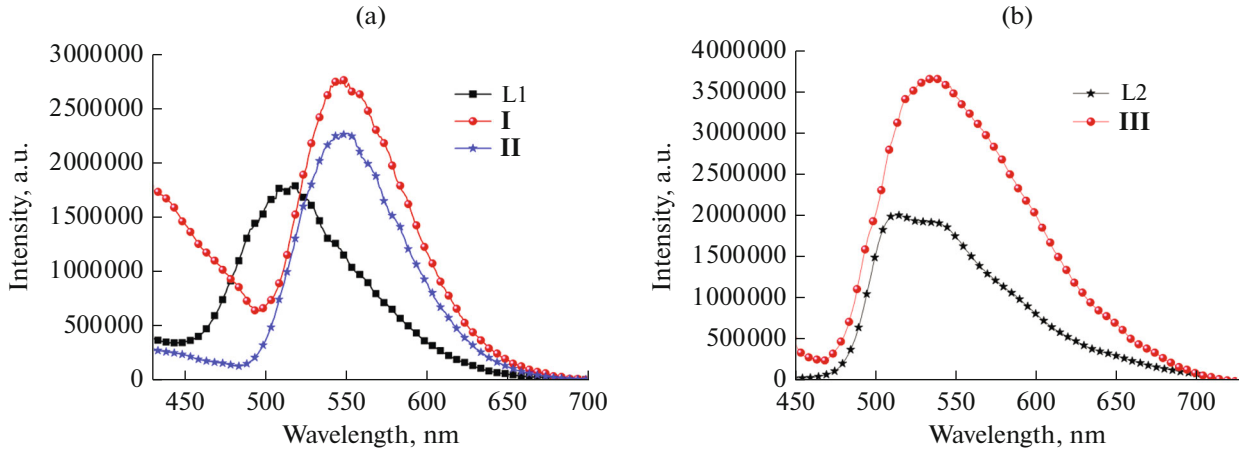

Fig. 4. Solid-state emission spectra of the organic ligands and complexes **I**–**III** at room temperature.

(1508085MB21), Doctoral Startup Foundation of Fuyang Normal College (FSB201501010), Students Research Training Program of Education Committee of Anhui Province (201510371040), National Students Research Training Program of China (201510371013, 201610371015)Research Innovation Team of Fuyang Normal College (kytd201710), and Natural Science Foundation of Education Committee of Anhui Province (2014KJ015).

REFERENCES

1. Yellol, G.S., Yellol, J.G., Kenche, V.B., et al., *Inorg. Chem.*, 2015, vol. 54, p. 470.
2. Baggaley, E., Weinstein, J.A., Williams, J.A.G., et al., *Coord. Chem. Rev.*, 2012, vol. 256, p. 1762.
3. Wang, J.C., Liu, Q.K., Ma, J.P., et al., *Inorg. Chem.*, 2014, vol. 53, p. 10791.
4. Jin, F., Pan, C.Y., Zhang, W.X., et al., *J. Lumin.*, 2016, vol. 172, p. 264.
5. Li, X.X., Gong, Y.Q., Zhao, H.X., et al., *Inorg. Chem.*, 2014, vol. 53, p. 12127.
6. Jin, F., Zhang, Y., Wang, H.Z., et al., *Cryst. Growth Des.*, 2013, vol. 13, p. 1978.
7. Jin, F., Wang, H.Z., Zhang, Y., et al., *CrystEngComm*, 2013, vol. 15, p. 3687.
8. Jin, F., Wang, H.Z., Zhang, Y., et al., *J. Coord. Chem.*, 2013, vol. 66, no. 20, p. 3686.
9. Xi, W.G., Yang, M.D., Wang, L.P., et al., *Russ. J. Coord. Chem.*, 2014, vol. 40, no. 10, p. 704.
10. Jin, F., Yang, X.F, Zheng, Z., et al., *CrystEngComm*, 2012, vol. 14, p. 8409.
11. Zhou, F.X., Zheng, Z., Zhou, H.P., et al., *CrystEngComm*, 2012, vol. 14, p. 5613.
12. Das, S., Nag, A., Goswami, D., et al., *J. Am. Chem. Soc.*, 2006, vol. 128, p. 403.
13. Gao, Y.H., Wu, J.Y., Zhou, H.P., et al., *J. Am. Chem. Soc.*, 2009, vol. 131, no. 14, p. 5208.
14. Hai, Y., Chen, J.J., Zhao, P., et al., *Chem. Commun.*, 2011, vol. 47, p. 2435.
15. Chen, Y.C., Bai, Y., Han, Z., et al., *Chem. Soc. Rev.*, 2015, vol. 44, p. 4517.
16. Jin, F., Sun, L., Liu, Y., et al., *Dyes. Pigm.*, 2015, vol. 121, p. 379.
17. Sheldrick, G.M., *SADABS, a Program for Exploiting the Redundancy of Area-Detector X-ray Data*, Göttingen: Univ. of Göttingen, 1999.
18. Jin, F., Hao, F.Y., Tian, Y.P., et al., *Chin. J. Struct. Chem.*, 2006, vol. 25, p. 1303.
19. Jin, F., Zhou, F.X., Yang, X.F., et al., *Polyhedron*, 2012, vol. 43, p. 1.
20. Li, Y.W., Ma, H., Chen, Y.Q., et al., *Cryst. Growth Des.*, 2012, vol. 12, p. 189.
21. Ooyama, Y., Yoshikawa, S., Watanabe, S., et al., *Org. Biomol. Chem.*, 2006, vol. 4, p. 3406.
22. Massin, J., Dayoub, W., Mulatier, J.C., et al., *Chem. Mater.*, 2011, vol. 23, p. 862.
23. Lee, Y.T., Chiang, C.L., Chen, C.T., et al., *Eur. J. Org. Chem.*, 2010, vol. 16, p. 3033.
24. Kippelen, B., Meyers, F., and Peyghambarian, N., *J. Am. Chem. Soc.*, 1997, vol. 9, no. 11, p. 4559.
25. Englert, B.C., Smith, M.D., Hardcastle, K.I., et al., *Macromolecules*, 2004, vol. 37, p. 8212.
26. Chun, H., Moon, I.K., Shin, D.H., et al., *Chem. Mater.*, 2001, vol. 13, p. 2813.
27. Jin, F., Zhu, H.Z., Tian, Y.P., et al., *J. Coord. Chem.*, 2014, vol. 67, no. 7, p. 1198.
28. Cheng, L., Cao, Q.N., Zhang, L.M., et al., *J. Coord. Chem.*, 2012, vol. 65, p. 1821.